Biogeosciences, 12, 2847–2860, 2015
www.biogeosciences.net/12/2847/2015/
doi:10.5194/bg-12-2847-2015

Biogeosciences
Open Access

Methane-related changes in prokaryotes along geochemical profiles in sediments of Lake Kinneret (Israel)

I. Bar-Or[1], E. Ben-Dov[2,3], A. Kushmaro[2,5,6], W. Eckert[4], and O. Sivan[1]

[1]Department of Geological and Environmental Sciences, Ben-Gurion University of the Negev, Be'er-Sheva, P.O. Box 653, 8410501, Israel
[2]Avram and Stella Goldstein-Goren Department of Biotechnology Engineering, Ben-Gurion University of the Negev, Be'er-Sheva, P.O. Box 653, 8410501, Israel
[3]Department of Life Sciences, Achva Academic College, Achva, M.P. Shikmim 79800, Israel
[4]Israel Oceanographic and Limnological Research, The Yigal Allon Kinneret Limnological Laboratory, P.O. Box 447, 14950 Migdal, Israel
[5]National Institute for Biotechnology in the Negev, Ben-Gurion University of the Negev, P.O. Box 653, Be'er-Sheva 8410501, Israel
[6]School of Materials Science and Engineering, Nanyang Technological University, Singapore

Correspondence to: A. Kushmaro (arielkus@bgu.ac.il)

Received: 27 May 2014 – Published in Biogeosciences Discuss.: 24 June 2014
Revised: 29 March 2015 – Accepted: 9 April 2015 – Published: 19 May 2015

Abstract. Microbial methane oxidation is the primary control on the emission of the greenhouse gas methane into the atmosphere. In terrestrial environments, aerobic methanotrophic bacteria are largely responsible for this process. In marine sediments, a coupling of anaerobic oxidation of methane (AOM) with sulfate reduction, often carried out by a consortium of anaerobic methanotrophic archaea (ANME) and sulfate-reducing bacteria, consumes almost all methane produced within those sediments. Motivated by recent evidence for AOM with iron(III) in Lake Kinneret sediments, the goal of the present study was to link the geochemical gradients in the lake porewater to the microbial community structure. Screening of archaeal 16S rRNA gene sequences revealed a shift from hydrogenotrophic to acetoclastic methanogens with depth. The observed changes in microbial community structure suggest possible direct and indirect mechanisms for the AOM coupled to iron reduction in deep sediments. The percentage of members of the *Nitrospirales* order increased with depth, suggesting their involvement in iron reduction together with *Geobacter* genus and "reverse methanogenesis". An indirect mechanism through sulfate and ANME seems less probable due to the absence of ANME sequences. This is despite the abundant sequences related to sulfate-reducing bacteria (*Deltaproteobacteria*) together with the occurrence of *dsrA* in the deep sediment that could indicate the production of sulfate (disproportionation) from S^0 for sulfate-driven AOM. The presence of the functional gene *pmoA* in the deep anoxic sediment together with sequences related to *Methylococcales* suggests the existence of a second unexpected indirect pathway – aerobic methane oxidation pathway in an anaerobic environment.

1 Introduction

Chemical profiles in the porewater of aquatic sediments reflect the sequence of microbially mediated redox reactions that are driven by the availability of both electron donors and of suitable electron acceptors. The latter are depleted in the order of decreasing chemical potential, beginning with oxygen and proceeding through nitrate, manganese and iron oxides, and then sulfate. Below the main zone of sulfate reduction, the fermentation of organic carbon leads to the formation of methane (CH_4) through methanogenesis (Froelich et al., 1979).

The produced methane is isotopically depleted in ^{13}C, with values of ~ -50 to -110 ‰ (Schoell, 1988), and the residual dissolved inorganic carbon (DIC) pool is enriched

by an isotopic fractionation factor (ε) of 50 to 70 ‰ (see, e.g., Borowski et al., 2000; Whiticar, 1999). When the produced methane diffuses into a zone with a suitable electron acceptor, it can be consumed by microbial oxidation (methanotrophy), the main process by which the important greenhouse methane is prevented from escaping into the atmosphere. While in the terrestrial environment, aerobic methanotrophy is the dominant process (Chistoserdova et al., 2005), in anaerobic marine sediments, archaea are found to consume the majority of upward-diffusing methane coupled to sulfate reduction (Knittel and Boetius, 2009; Thauer, 2010; Valentine, 2002).

Evidence from lipids and from fluorescence in situ hybridization (FISH) showed that a consortium of archaea and sulfate-reducing bacteria are involved in this anaerobic methane oxidation (AOM; Boetius et al., 2000; Hinrichs et al., 1999; Orphan et al., 2001). To date, three groups of anaerobic methanotrophic archaea (ANME), named ANME-1, ANME-2, and ANME-3, are known to perform sulfate-driven AOM (Niemann et al., 2006; Orphan et al., 2002). Recently, Milucka et al. (2012) demonstrated AOM mediated solely by archaea, where the archaea were shown to oxidize the methane and reduce the sulfate to elemental sulfur. Disproportionating bacteria, also involved in this mechanism, oxidize and reduce this elemental sulfur to sulfate and sulfide, respectively. The carbon isotopic fractionation factor (ε) for this methanotrophic process was shown to be in the range of 4–30 ‰ (Kinnaman et al., 2007; Whiticar, 1999). Enrichment cultures of ANME from different environments showed a carbon isotopic fractionation of 12–39 ‰ (Holler et al., 2009).

Other electron acceptors were recently shown to drive AOM. Nitrite-driven AOM through oxygenic bacteria was observed in two different freshwater ecosystems in the Netherlands (in canal sediments) (Ettwig et al., 2009; Raghoebarsing et al., 2006) and also in peatlands (Zhu et al., 2012). Beal et al. (2009) showed the potential of manganese- and iron-driven AOM in marine sediments, and Egger et al. (2015) showed it in brackish costal sediments. In our recent study (Sivan et al., 2011), we provided in situ geochemical evidence for AOM coupled to microbial iron reduction below the main methanogenesis zone in Lake Kinneret (LK) sediments, where dissolved sulfate and nitrate are absent. However, the mechanism that is responsible for this process was not investigated. The goal of the present study is to explore the possible microbial communities that may be involved in the iron-driven AOM in LK sediments. This is accomplished by combining chemical and isotope analyses of porewater samples along a depth profile from LK sediments with molecular biological techniques. By using specific functional genes related to dissimilatory sulfate reductase (*dsr*) for sulfate reducers (Klein et al. 2001), methyl-coenzyme M reductase (*mcr*) for methanogens and anaerobic methanotrophs (Hallam et al., 2003) and particulate methane monooxygenase (*pMMO*) for aerobic methanotrophs (McDonald et al., 2008), we pinpoint the most likely candidate for this relatively unknown process.

2 Study site

Located in northern Israel, Lake Kinneret (LK, Fig. 1) is a warm monomictic subtropical lake. Typical concentrations of major electron acceptors in the water column during the mixed period are 35–50 µM nitrate and 600 µM sulfate (Adler et al., 2011; Nishri et al., 2000; Serruya et al., 1974). In the spring, the newly formed epilimnion is characterized by increasing temperatures and enhanced phytoplankton development, while in the hypolimnion heterotrophic microorganisms gradually deplete oxygen and then nitrate. Organic matter degradation by bacterial iron and manganese reduction takes place below the thermocline in the summer; at the end of the stratification period, sulfate reduction starts in the bottom water. In the upper part of the sediment, sulfate reduction is the dominant microbial process year round, and below depth of 5 cm this process is mostly replaced by methanogenesis (Adler et al., 2011; Eckert and Conrad, 2007). Total iron content ($Fe_{(tot)}$) in the sediment increases with depth till 18 cm and then remains uniform around 550 µmol g^{-1} dry weight (Eckert, 2000). Mn(II) concentration is about 13 µmol g^{-1} dry weight in the sediment (Serruya, 1971). The total carbon (C_{tot}) in the solid phase shows a decrease from 14 µmol g^{-1} dry weight in the top part of the sediment to 8 µmol g^{-1} dry weight in the deep part of the sediment ($\sim$ 30 cm; Eckert, 2000).

3 Material and methods

3.1 Sampling

Several sediment cores were collected from the center of the lake (Station A, Fig. 1) at a water depth of $\sim$ 42 m (maximum lake water column depth) at different times using Perspex tubes, measuring 55 cm long by 5 cm in diameter, with a gravity corer. The cores were stored in the dark at 4 °C until they were sliced (on the same day or the day after). Core sampling for the microbial community study took place in December 2009. Over a dozen porewater chemical and isotope profiles were conducted seasonally (every 3–4 months) from 2007 to 2013. The slight seasonal changes allowed the use of typical geochemical profiles (Adler et al., 2011) in order to sample for the microbiology communities in the different electron acceptors zones and to find correlations between the microbial sampling and the geochemical profiles.

3.2 Geochemical analyses

Cores were divided into 2 cm slices from top to bottom under a constant flow of N_2 using a slicing device (Eckert, 2000). About 1.5 mL of each sediment slice was transferred into N_2-

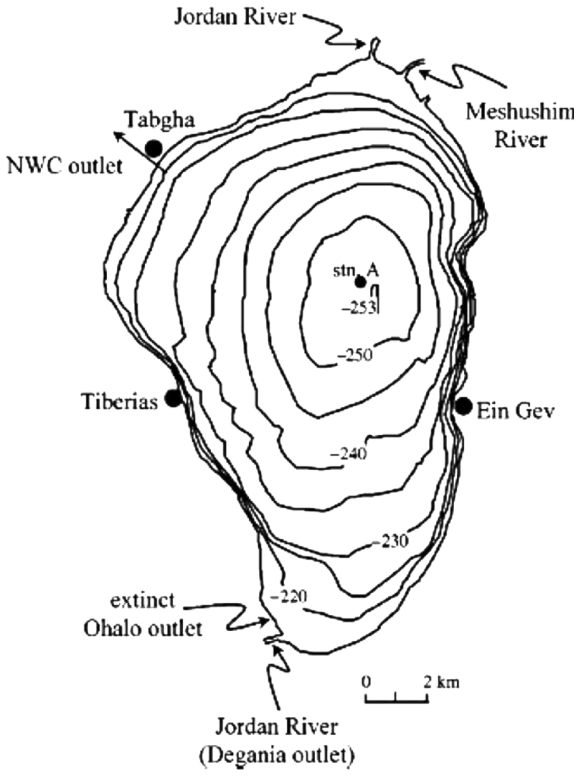

Figure 1. Map of Lake Kinneret, located in the north of Israel. Numbers correspond to altitude measured in meters from the level of Lake Kinneret. Cores were taken from station A (taken from Hambright et al., 2004).

flushed crimp bottles containing 5 mL of 1.5 N NaOH for the headspace measurements of CH_4 and $\delta^{13}C_{CH_4}$ (after Sivan et al., 2011). CH_4 concentrations were measured on a SHIMADZU gas chromatograph (GC 8IF) equipped with a flame ionization detector (FID) at a precision of 2 µmol L^{-1}.

Porewater was extracted immediately from each slice by centrifugation at 27 000 g at 4 °C in a N_2 atmosphere, and the supernatant was filtered through 0.45 µm filters. A 1 mL subsample was fixed with ferrozine and analyzed for dissolved Fe(II) (Stookey, 1970). Four millimeters of subsample was poured into an acidified vial (1 mL of 0.5 N nitric acid) to measure dissolved Mn(II). The sample was analyzed via an inductively coupled plasma mass spectrometer (ICP-MS, Elan DRC II, Perkin Elmer) at a precision of ±10 %. For sulfide profiles, 1 mL of subsample was added to zinc acetate, and hydrogen sulfide concentrations were determined by the methylene blue method, where the MDL (method detection limit) is 1 µM (Cline, 1969). For sulfate measurements, 5 mL of the subsamples was analyzed with a Dionex DX500 high-pressure liquid chromatograph with a precision of ±3 %. Iron isotope analysis was done by acidifying the subsamples with 10 % HCl for 1 week (to dissolve any precipitated iron) and then purifying them through anion exchange chromatography (Borrok et al., 2007). δ^{56}Fe was measured on a Neptune multi-collector ICP-MS in high-resolution mode according to standard methods and standardized against isotopic reference material (IRMM-014) with a precision of ±0.1 ‰ (John and Adkins, 2010). Total lipids were extracted using the Bligh–Dyer procedure (Bligh and Dyer, 1959) with solvent mixture of 2 : 1 : 0.8 (methanol : dichloromethane : buffer). δ^{13}C of the total lipid extraction (TLE) was measured on an elemental analyzer–isotopic ratio mass spectrometer (EA-IRMS) with a precision of 0.1 %.

3.3 DNA extraction and quantitative PCR (qPCR) amplification from sediment samples

Part of the sediment slices were kept frozen at −20 °C for the microbial work. Samples from three different depths (0–3 cm representing the sulfate reduction zone, 6–9 cm representing the methanogenesis zone and 29–32 cm representing the deep AOM zone) were defrosted. Those depth zones were chosen based on the geochemical profiles sampled at different times, showing quasi-steady state and stabilization of the sediments (Adler et al., 2011; Sivan et al., 2011). Therefore, microbial community sampling of the three depth zones at a single point in time should represent the different microbial habitats as they pertain to the respective geochemical zones. Total genomic DNA was extracted from the sediment samples using the MO BIO PowerSoil DNA Isolation Kit (MO BIO Laboratories, Solana Beach, CA). Genomic DNA was eluted using 60 µL of elution buffer and stored at −20 °C. Concentrations of DNA were determined via UV–visible spectrophotometry (ND-1000 NanoDrop Technologies, Wilmington, DE; sulfate reduction zone 22, methanogenesis zone 35.8 and AOM zone 14 ng μL^{-1}).

Quantification of functional genes was performed using *mcrA* primers (Luton et al., 2002), Forward ′GGTGGTGTMGGATTCACACARTAYGCWACAG′ and Reversed ′TTCATTGCRTAGTTWGGRTAGTT′, *dsrA* primers, DSR1F ′ACSCACTGGAAGCACG′ (Wagner et al., 1998) and RH3-dsr-R ′GGTGGAGCCGTGCATGTT′ (Ben-Dov et al., 2007) and *pmoA* primers, a189F ′GGNGACTGGGACTTCTGG′ and mb661R ′CCGGMGCAACGTCYTTACC′ (Yan et al., 2006) with an ABI PRISM 7000 Sequence Detection System (Applied Biosystems). The qPCR reaction consisted of 10 µL of ABsolute Blue SYBR Green ROX, 150 nM each of forward and reverse primers and 5 µL of each DNA template. Thermal cycling conditions were as follows: 15 min at 95 °C for enzyme activation, followed by 40 rounds of 15 s at 95 °C for denaturation and 1 min at 60 °C for annealing/extension. To verify that the used primer pair produced only a single specific product, a dissociation protocol was added after thermocycling to determine dissociation of the PCR products from 60 to 95 °C. Standards for the calibration curves for quantification were made using pGEM-T Easy plasmid cloned with 1.9 kb *dsrA* and amplicons of the *mcrA* and *pmoA* encoding for functional genes at a known concen-

tration with six serial dilution points (in steps of 10-fold). All runs included a no-template control. Plasmid standards and environmental samples were simultaneously assayed in triplicates. The ABI PRISM 7000 Sequence Detection System and SDS Software were used for data analysis. QC (quality control) values were exported into a Microsoft Excel worksheet for further statistical analysis.

3.4 Sequence analysis

454 tag-encoded amplicon pyrosequencing was performed by the Research and Testing Laboratory (Lubbock, Texas, USA) as previously described (Dowd et al., 2008). The bacterial and archaeal 16S rRNA gene primers that were used are 28F ′GAGTTTGATCNTGGCTCAG′ and 519R ′GTNTTACNGCGGCKGCTG′, and Arch349F ′GYGCASCAGKCGMGAAW′ and Arch806R ′GGACTACVSGGGTATCTAAT′, respectively.

Data analysis was made using two different methodologies (MOTHUR and SILVA ngs). The initial trimming of the sequences was made by MOTHUR v1.33 (Schloss et al., 2009) and generated around 300 bp of sequences. The trimmed sequences were taken to further analysis by MOTHUR (Schloss et al., 2011) using SILVA NR v119 database. MOTHUR 454 pipeline filtration and denoising sequences remove from the analysis that were < 150 bp, when they contained homopolymers longer than 8 bp, ambiguous bases, more than one mismatch to barcode sequences or more than two mismatches to the forward primer sequence. We further removed sequences that did not align in the same nucleotide position on the reference database.

Most of the bacterial sequences were in the same region; however, the archaeal sequences were spaced between two different regions. We used one position window that was dominant in the top sample and implied it to the other archaeal analysis in order to better compare the data set between other samples of the same position window. Identical sequences were grouped and then were aligned against SILVA.nr_v119. Chimeras were removed using MOTHUR CHIMERA UCHIME (Edgar et al., 2011). The lengths of the remaining sequences were around 200 bp. A further screening step (pre-cluster) was applied to reduce sequencing noise by clustering reads differing by only 1 base every 100 bases (Huse et al., 2010). In addition, the rest of the sequences were classified in order to remove eukaryote, mitochondria and chloroplast classified sequences. The remaining sequences were used to generate a distance matrix and clustering into operational taxonomic units (OTUs) defined at 97 % cutoff using the average neighbor algorithm. The OTUs were classified using the SILVA.nr_v119 database with a confidence threshold of 80 %. Alpha diversity was calculated by MOTHUR using the remaining sequences at 97 % similarity. The beta diversity was calculated using comparable data; the number of sequences per sample was made equal through subsampling (Tables 1 and 2).

The second program which we used for analysis was SILVA ngs pipeline (Quast et al., 2013). The trimmed sequences from MOTHUR were Aligner against the SILVA SSU rRNA seed. Sequences shorter than 50 aligned nucleotides and with more than 2 % of ambiguities or 2 % of homopolymers, respectively, were removed. The sequences that were not aligned as being putative contaminations/artifacts were removed. Then sequences were clustered to OTUs with 98 % similarity and classified by local nucleotide BLAST search against SILVA database v119. To filter out low identity and artificial BLAST hits, hits for which the function (% sequence identity + % alignment coverage)/2 did not exceed the value of 93 % were discarded. Sequences with weak, low scores were classified as "No Relatives" and were disregarded thereafter. Standard deviation betweena the percentages of the two classification showed that at the phylum level there are small differences between the two pipelines (Table S1 in the Supplement). In the order classification, the standard deviations increased but the sequences still showed close similarity. Estimates of phylotype richness, diversity coverage and similarity were calculated according to the abundance-based coverage estimate (ACE), Chao's estimator (Chao, 1984; Chao and Ma, 1993), the Shannon diversity index, and Good's coverage (Good, 1953) in MOTHUR (Tables 1 and 2). The distribution and abundance matrix of the OTUs was normalized to the sample with the smallest number of reads by randomly resampling the MOTHUR data set for statistical comparisons. Raw sequencing data were deposited in the MG-RAST (metagenomics.anl.gov) archive.

3.5 Microbial community structure related to the environment conditions

To estimate community similarity among samples, we used PC-ORD 6 software. Subsample OTU data from MOTHUR was used to create a distance matrix based on the Sørensen (Bray–Curtis) dissimilarities of the OTU composition of the samples. The data were normalized to percentages before the analysis. Community relationships were visualized using principal coordinate analysis (PCoA) based on this distance matrix. Different environmental variables were added as well (CH_4, $\delta^{13}C_{CH_4}$, Fe(II), δ^{56}Fe(II), Mn(II), H_2S, SO_4^{2-}, dissolved organic carbon (DOC), $\delta^{13}C_{TLE}$, NH_4^+ and PO_4^{3-}) in order to identify potential explanatory variables. The environmental vectors were applied and projected to the PCoA ordination. In addition, Venn diagrams for graphical descriptions of unshared and shared OTUs among the three samples were constructed using MOTHUR.

4 Results

4.1 Porewater profiles

This study focused on microbial community shifts along the porewater profiles of electron acceptor gradients related to

Table 1. Bacterial sequences used for classification in SILVA ngs and for subsample in MOTHUR for the alpha diversity.

Bacteria	# seq SILVA ngs	OTUs SILVA ngs	# seq MOTHUR	OTUs MOTHUR	Good's coverage	invSimpson	Chao	Ace	Shannon
0–3 cm	3631	599	2588	388	0.92	10/10.8/11.7	805/925.7/1092.8	1246.5/1384.0/1546.7	3.83/3.91/3.98
6–9 cm	4641	1735	3365	1337	0.77	286.6/315.9/351.8	2437.9/2673.0/2958.4	3876.8/4135.2/4420.0	6.48/6.53/6.57
29–32 cm	5038	1516	3615	1214	0.81	127.8/142.4/160.6	2104.4/2318.7/2583.1	3047.7/3259.5/3495.4	6.13/6.19/6.24

Table 2. Archaeal sequences used for classification in SILVA ngs and for subsample in MOTHUR for the alpha diversity.

Archaea	# seq SILVA ngs	OTUs SILVA ngs	# seq MOTHUR	OTUs MOTHUR	Good's coverage	invSimpson	Chao	Ace	Shannon
0–3 cm	288	48	268	32	0.90	2.5/2.9/3.5	53.9/83.4/164.5	232.8/344.6/520.4	1.6/1.8/2.0
6–9 cm	1382	184	1408	200	0.86	8.4/10.2/13.2	39.0/131.4/220.4	144.7/195.2/277.4	2.87/3.05/3.22
29–32 cm	3110	383	2829	245	0.88	7.9/9.2/10.9	73.5/104.8/181.7	133.2/190.9/289.6	2.58/2.74/2.91

the methane cycle. To characterize shifts in main electron acceptors with depth, over a dozen porewater profiles were performed seasonally from station A (Fig. 1). The shown profiles (Fig. 2) are representatives of the slight seasonal trends. Sulfate and sulfide profiles show depletion from $\sim 100\,\mu M$ at the top part of the sediment, to below detection limits within the upper 15 cm (Fig. 2a). This typical concave curvature profile of the sulfate profile in the porewater indicates intensive sulfate reduction in the upper few centimeters of the sediment throughout the year. A typical LK methane concentration profile (Fig. 2b) shows increase from 250 µM at the water–sediment interface to a maximum of about 1.25 mM in the depth range of 7 to 15 cm, and then a decrease below 15 cm depth. The profile of $\delta^{13}C_{CH_4}$ (Fig. 2b) shows a decrease from −60 ‰ at a depth of 1 cm to about −65 ‰ at a depth of 7 cm and then an increase in the deeper sediments to a maximum value of −53.5 ‰ at a depth of 25 cm. Also, the profile of $\delta^{13}C_{TLE}$ (Fig. 2c) shows a decrease in this deepest part of the sediment.

Manganese and iron oxides are the most probable electron acceptors in the deeper part of the sediment where methane is decreased. Dissolved Mn(II) concentration (Fig. 2d) increased from 5 µM at the top of the sediment to a plateau of about 23 µM from depths of 23 to 36 cm. The dissolved Fe(II) concentration profile also showed an increase with depth (Fig. 2d), although following a different pattern. In the upper 15 cm, dissolved Fe(II) concentrations were below the detection limit, and gradually increased below 15 cm to about 90 µM at a depth of 36 cm. The δ^{56}Fe profile (Fig. 2c) showed a decrease with depth from 0.5 ‰ in the upper part to −1.7 to −2.3 ‰ in the deeper part of the sediment.

4.2 Sediment microbial communities

To study the sediment depth-dependent microbial community shifts, 16S rRNA gene sequences of the prokaryotic community from three different depth zones (0–3, 6–9 and 29–32 cm, see arrows in Fig. 2a) were extracted and analyzed. As mentioned above, these three zones represent the main sulfate reduction zone, the methanogenesis zone and the deep iron-driven AOM zone, respectively. The diverse bacterial and archaeal communities at these depth zones varied in composition and richness throughout the sediment. A total of 13227 and 4881 bacterial and archaeal sequences, representing 3852 and 705 OTUs (cut-off value of 98 %), respectively, were identified by the SILVA database project. The normalized Shannon and Chao index were used as proxies for diversity and richness, respectively (Tables 1 and 2). The upper layer showed lower diversity (Shannon index, 3.91 and 1.8 for bacteria and archaea) and richness (Chao index, 925.7 and 83.4 for bacteria and archaea) than the other depths. Moreover, the bacterial coverage of the upper layer was the highest (91 %), while that of the deeper layers was about 80 %. The archaeal coverage was almost the same ($\sim$ 88 %) in all the sampled layers. Most of our sequences were affiliated with uncultured microorganisms mainly from various sediment environments.

Although the bacterial OTUs were distributed over 43 phyla, we present here only the phyla that were over 1 % sequences of the 454 library. The most abundant phyla were *Proteobacteria*, *Chloroflexi*, *Nitrospirae*, *Bacteroidetes*, *Firmicutes* and *Chlorobi* observed in at least one of the libraries (Fig. 3).

The communities of microorganisms in the top layer (0–3 cm) of the sediment had less sequence overlap with those of the deeper layers (70 and 33 shared bacterial sequences with the middle and bottom layers, respectively) and of the deeper layers (Figs. S1 and S2 in the Supplement). The most dominant ($\sim$ 48 %) phylum in this bacterial community was *Proteobacteria*; class *Gammaproteobacteria* (91 %) and the genera *Acinetobacter* (28 %) and *Pseudomonas* (14 %; Fig. 3). The second most abundant (38 %) phylum was *Firmicutes*; class *Clostridia* (21 %) and *Bacilli* (17 %), family *Clostridiaceae* (15 %) and genus *Bacillus* (14 %). Further sequences were related to other phyla and orders (Fig. 3 and Table S1).

In the archaeal community, the sequence numbers were much lower, although the coverage calculation shows about 90 % coverage. The dominant phylum in the upper layer

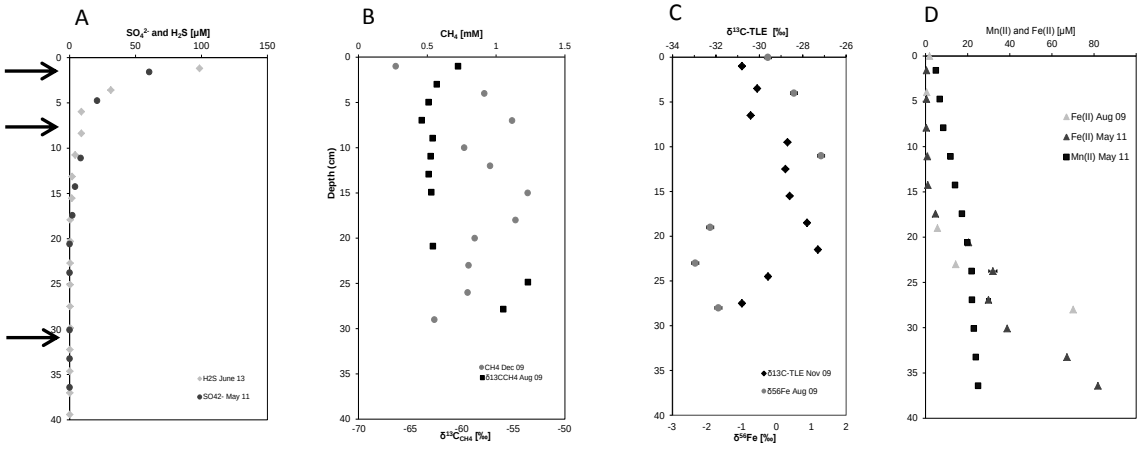

Figure 2. Geochemical porewater profiles in LK sediment. **(a)** Profile of SO_4^{-2} (black circles) and sulfide (gray diamonds) in the porewater **(b)**. Headspace measurements of methane (gray circles) and $\delta^{13}C_{CH_4}$ (black squares) in the sediments **(c)** $\delta^{13}C$ of total lipids extraction (TLE; black diamonds) from the sediment, and $\delta^{56}Fe$ (gray circles) of the dissolved iron in the porewater. **(d)** Electron acceptor profiles of dissolved Fe(II) (gray triangles) and Mn (II) (black squares) in the porewater. Black arrows indicate the sampled sections for 16S rRNA gene analysis. The presented methane profile was taken 2 weeks prior to the sampling for the microbial communities on December 2009. Sampling for Fe(II), Mn(II) and SO_4^{-2} profiles was carried out between 2007 and 2011 and for sulfide between 2007 and 2013. The $\delta^{13}C_{CH_4}$ and $\delta^{56}Fe$ profiles were performed 4 months prior to the microbial sampling on August 2009.

was *Euryarchaeota* (98 %), and the other 2 % was *Thaumarchaeota*. *Methanomicrobia* (92 %) was the dominant class of *Euryarchaeota* divided among genera of *Methanoregula* (58 %), *Methanosaeta* (22 %) and *Methanolinea* (11 %). The other abundant classes of *Euryarchaeota* were *Halobacteria* (2 %) and *Thermoplasmata* (3 %). Marine Benthic Group B (MBG-B 0.7 %) and Miscellaneous Crenarchaeotic Group (MCG 1 %; Fig. 4 and Table S1).

The middle layer (6–9 cm) was the richest and most diverse in its bacterial and archaeal populations comparing to the other layers, but with the lowest community coverage (bacterial 77 and archaeal 86 %). The dominant phyla in this depth were divided into *Proteobacteria* (40 %), *Chloroflexi* (14 %), *Bacteroidetes* (7 %), *Chlorobi* (5 %) and *Nitrospirae* (4 %). The dominant classes in *Proteobacteria* were *Deltaproteobacteria* (68 %), *Betaproteobacteria* (14 %) and *Gammaproteobacteria* (14 %). Sva0485 (8 %), *Syntrophobacterales* (7 %), *Desulfarculales* (3 %) and *Desulfuromonadales* (2 %) were the affiliated dominant orders in *Deltaproteobacteria*. The *Methylococcaceae* family of *Gammaproteobacteria* comprised 1 % of affiliated sequences. The dominant family in *Chloroflexi* was *Anaerolineaceae* (6 %). The *Ignavibacteriales* (4 %) order was dominant in *Chlorobi*. *Nitrospirae* increased from the upper layer and was mainly represented by the *Nitrospiraceae* (4 %) family. Further sequences were related to other phyla and orders (Fig. 3, Table S1).

The archaeal community was the richest and most diverse in the middle zone. The dominant phyla were *Euryarchaeota* (96 %), while *Thaumarchaeota* comprised the other 4 %. *Euryarchaeota* was divided among three dominant classes: *Methanomicrobia* (78 %), *Thermoplasmata* (11 %) and *Halobacteria* (6 %). *Methanomicrobia* was divided among *Methanoregula* (19 %), *Methanosaeta* (50 %) and *Methanolinea* (10 %) genera. *Thermoplasmata* was divided between Marine Benthic Group D (5 %) and Terrestrial Miscellaneous Group (TMEG; 3 %). The dominant *Halobacteria* family was Deep Sea Hydrothermal Vent Group 6 (DHVEG-6; 6 %), Marine Benthic Group B (MBGB 1.5 %) and Miscellaneous Crenarchaeotic Group (MCG 1.5 %; Fig. 4 and Table S1).

The dominant phyla in the bottom layer (29–32 cm) bacterial community included *Proteobacteria* (39 %), *Chloroflexi* (19 %) and *Nitrospirae* (8 %). *Proteobacteria* were divided into three main classes: *Deltaproteobacteria* (20 %), *Gammaproteobacteria* (10 %) and *Betaproteobacteria* (6 %). Sva0485 (11 %) and *Syntrophobacterales* (4 %) were the affiliated dominant orders in *Deltaproteobacteria*. The dominant family in *Chloroflexi* was *Anaerolineaceae* (7 %), and the *Ignavibacteriales* (4 %) order was the dominant *Chlorobi*. *Nitrospirae* increased from the upper layer and was mainly represented by the *Nitrospiraceae* (8 %) family. Further sequences were related to other phyla and orders (Fig. 3, Table S1).

At this depth, the dominant archaeal phyla were *Euryarchaeota* (98 %) while *Thaumarchaeota* comprised the other 2 %. *Euryarchaeota* was divided among three dominant classes: *Methanomicrobia* (86 %), *Thermoplasmata* (6 %) and *Halobacteria* (5 %). *Methanomicrobia* was divided among *Methanoregula* (16 %), *Methanosaeta* (58 %) and *Methanolinea* (11 %) genera. *Thermoplasmata* was divided among Marine Benthic Group D (MBG-D; 5 %)

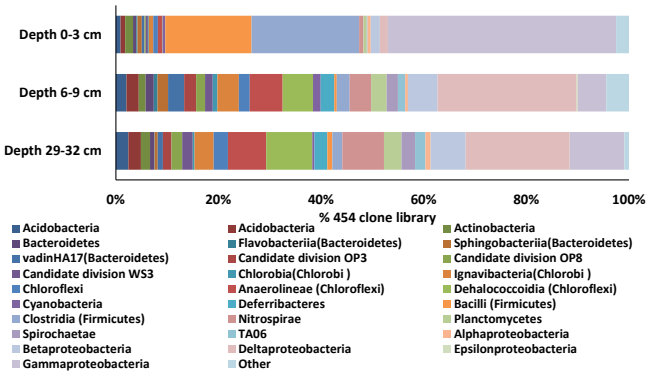

Figure 3. Classification of bacterial sequences using SILVA ngs pipeline. Phyla and class distributions of sequences of the 454 sequencing above 1 % at the different depths in the communities.

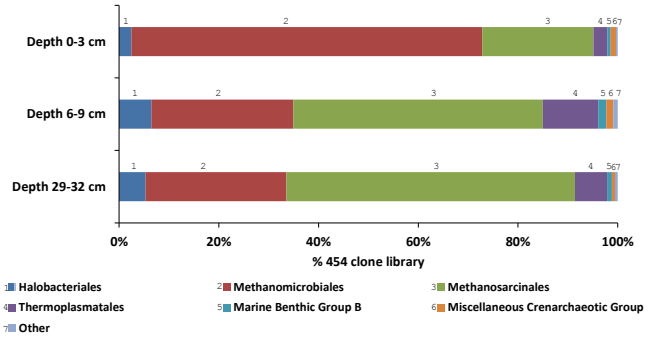

Figure 4. Classification of archaeal sequences using SILVA ngs pipeline. Phyla and order distributions of sequences of the 454 sequencing above 1 % at the different depths in the communities.

and Terrestrial Miscellaneous Group (TMEG; 3 %) families. The dominant *Halobacteria* family was Deep Sea Hydrothermal Vent Group 6 (DHVEG-6; 1 %), Marine Benthic Group B (MBG-B 1 %) and Miscellaneous Crenarchaeotic Group (MCG 0.6 %; Fig. 4 and Table S1). A detailed description of the major communities in the sediment is described in the Discussion section and the Supplement. No ANME sequences were detected even though specific primers (ANME2C-AR468F, ANME3-1249, ANME1-395F, ANME1-1417, ANME3-140F, ANME3-1249, ANME2a-426 and ANME2a-1242R, see Miyashita et al., 2009) were used.

4.3 Depth comparison of microbial communities

An ordination plot from the 454 pyrosequencing by MOTHUR subsample OTUs data set was derived from principal coordinate analysis (PCoA) of the bacterial and archaeal. The PCoA display the similarities and differences between the bacterial and archaeal communities varied with depth (Fig. 5a and b, respectively). The PCoA of bacteria and archaea show very similar separation among the communities of different layers related to the different environment conditions of each layer. The two deeper layers are on the same point along the x axis, showing relatively more similarity than the upper layer. The vectors of the sulfate and sulfide are correlative with communities of the top layer, while methane, $\delta^{13}C_{TLE}$ and $\delta^{56}Fe(II)$ were more associated with the communities of the middle layer. The communities in the bottom layer were more correlated to Fe(II), Mn(II) and NH_4^+. The Venn diagram shows also that more OTUs from the deeper layers were shared than between the upper layer and the deeper layers (Figs. S1 and S2).

4.4 Functional gene profile

In order to better understand the abundance of microbial functionality at different depths, we used qPCR for different functional genes. The functional genes *mcrA* and *dsrA* had a very similar pattern – low concentrations in the upper layer ($9 \times 10^5 \pm 6.4 \times 10^4$ and $1 \times 10^6 \pm 1.7 \times 10^5$, respectively) and highest concentrations ($6.9 \times 10^6 \pm 6.7 \times 10^5$ and $6.9 \times 10^6 \pm 9.9 \times 10^4$) in the middle layer. The *pmoA* gene showed also the same pattern, although with lower concentrations ($2.3 \times 10^5 \pm 9.7 \times 10^3$ to $1.6 \times 10^6 \pm 1.7 \times 10^5$; Fig. 6).

5 Discussion

In this study of LK sediments, we investigated changes in the microbial diversity associated with porewater geochemistry and the transition of the dominant electron acceptors with depth (0–40 cm). The geochemical porewater profiles in LK (Fig. 2) suggest that the sediment can be broadly divided into three different regions of microbial processes: the upper 5 cm which is dominated by sulfate reduction, the methanogenesis zone between 5 and 17 cm, and the deep sediments, dominated by anaerobic oxidation of methane coupled to iron reduction. This division of the sediment and the deep iron-driven AOM processes were confirmed by in situ profiles of methane, $\delta^{13}C_{CH_4}$, sulfate, ferrous iron and subsequent use of a numerical mass conservation model (based on the geochemical profiles of DIC and $\delta^{13}C_{DIC}$; Adler et al., 2011) and a set of geochemical incubation experiments conducted in our previous work (Sivan et al., 2011).

The mechanisms that enable the process of AOM via iron reduction can be characterized by the existence of specific prokaryotic populations at each depth and their resemblance to similar environments with a distinct characterization. There are only a few studies that analyzed microbial communities relative to geochemical zones in freshwater sediments (Deutzmann and Schink, 2011; Koizumi et al., 2004; Ye et al., 2009). Therefore, this study can deepen knowledge of microbial community shifts under different electron acceptors conditions, especially those related to the methane cycle. It is also the first study in LK that divides the

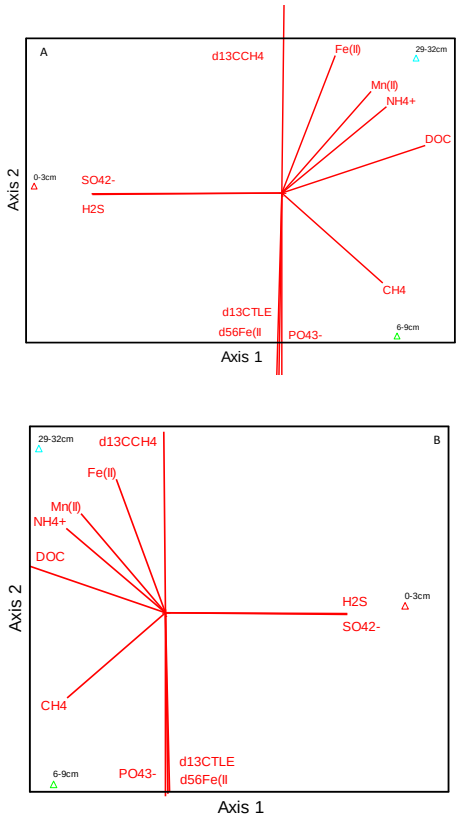

Figure 5. Principal coordinate analysis (PCoA) of the **(a)** bacterial and **(b)** archaeal community matrix (based on operational taxonomic units) and vector fitting of the environmental geochemical conditions in the different depth. The bacterial community from the upper layer is labeled with a red triangle, the middle layer is labeled with a green triangle and bottom layer is labeled with a blue triangle.

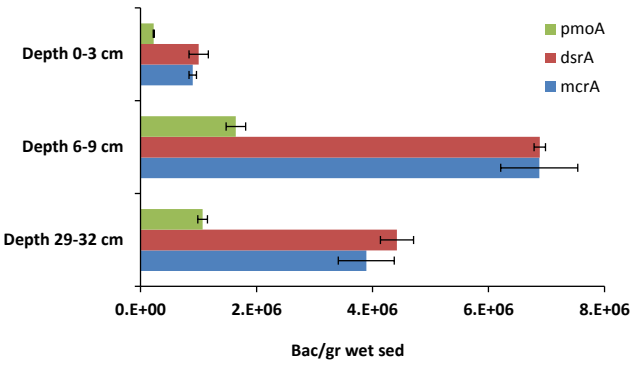

Figure 6. Profiles of functional genes from the three different depths. Green bars represent the *pmoA* functional gene of aerobic methanotroph, red bars represent the *dsrA* functional gene of sulfate reducers and blue bars represent the *mcrA* functional gene from methanogens and anaerobic methanotrophs.

sediment into different layers and contributes significantly to the understanding of the diversity of microbial ecology in different zones.

Pipeline of SILVA ngs was used for the alpha diversity to get more classified sequences and better coverage of the classification and population. However, for beta diversity the data from the MOTHUR pipeline were applied to get more statistical results without the bias of different sample size. The changes between the pipeline results for the alpha diversity were not large at the phyla level (standard deviation of $\sim 0.5\,\%$) but increased with higher taxonomy levels.

5.1 Sediment geochemical conditions

In the upper layer of sediment (0–3 cm), sulfate concentrations were the highest and decreased with depth as particulate organic matter from the water column accumulates, making organic carbon degradation available (Hadas and Pinkas, 1992). Adler et al. (2011) calculated that the bulk of bacterial sulfate reduction occurs in the top 1 cm of sediment, a finding that was supported by the microbial work of Hadas and Pinkas (1992). Using sulfide and particulate organic carbon measurements, Eckert and Conrad (2007) showed that sulfate reduction accounts for most of the mineralization of organic matter in the upper 15 cm of sediment. Methane concentrations in the upper layer were relatively low and probably occurred from upward diffusion as methanogens are outcompeted by sulfate reducers there (Lovley and Klug, 1983). The depletion in methane concentrations, decline of $\delta^{13}C_{TLE}$ values and the heavier isotopic values of $\delta^{13}C_{CH_4}$ in the upper layer (Fig. 2) compared to the methanogenic zone may be explained by AOM via sulfate reduction, although no ANME sequences were found using specific primers and fluorescence in situ hybridization methods or by our phylogenetic alignment of 16S rRNA gene libraries at any depth in the sediment.

Below the sulfate reduction zone, in the middle layer of sediment (6–9 cm), methane reached its maximum concentrations (Fig. 2b). The low values of $\delta^{13}C_{CH_4}$ in the methanogenesis zone are typical due to the large carbon isotope fractionation that occurs during methane production, thereby leaving the produced methane isotopically light and the DIC isotopically heavy. Below the maximum methane production zone (around 20 cm), methane concentrations began to decrease while $\delta^{13}C_{CH_4}$ values increased (Fig. 2b), an outcome that may be due to the AOM process, which leaves residual methane isotopically heavier. Depleted $\delta^{13}C_{TLE}$ (Fig. 2c) in the deeper part of the sediment also supports the presence of AOM with the production of light biomass from methane oxidation. In addition, although all the suitable electron acceptors at this depth were depleted, both Fe(II) and Mn(II) increased (Fig. 2d). Also, δ^{56}Fe values (Fig. 2c) of dissolved iron in the deeper part of the sediment were isotopically negative, similar to sediments with active dissimilatory bacterial iron reduction (Severmann et al., 2006) and are an indication of active iron reduction in the deep sediments and not

just diffusion. The increase in Fe(II) concentrations below a depth of 15 cm was probably supported by the absence of sulfide. The potential of highly reactive Fe(III) oxides to drive AOM in LK was also supported by our set of mesocosm incubation studies (Sivan et al., 2011). Since manganese oxide concentrations were very low ($\sim 0.04\,\%$) throughout the LK sediment column (Serruya et al., 1974), iron oxide seemed to play a bigger role in this AOM process.

5.2 Concept for methane cycle mechanisms

A few possible mechanisms for the novel process of iron-driven AOM in the deep part of the sediment can be suggested based on the geochemical profiles and the microbial communities. A possible direct process could be through new, currently unknown bacteria/archaea that reduce iron and utilize methane. Indirect processes could include (1) reduction of Fe(III) oxides through the oxidation of sulfide (in pyrite or FeS minerals) to sulfur intermediates, and then disproportionation to sulfide and sulfate (such as in Holmkvist et al., 2011; Sivan et al., 2014), and/or sulfate-driven AOM but without ANME; (2) reduction of Fe(III) by utilizing H_2 (Lovley, 1991), which could consume most of produced H_2 in the deep sediment. Thus creating a low concentration of H_2 which drives methanogenesis backwards ("reverse methanogenesis", Hallam et al., 2004; Hoehler et al., 1994) through methanogens in the deep sediment; (3) an oxygenic methane oxidation pathway in an anaerobic environment as described by Ettwig et al. (2010), when methane is oxidized by oxygen that is released from iron oxides.

Changes in the microbial population shown in the present study may support the deep iron-driven AOM mechanism (presented by the sample from 29–32 cm). The bacterial diversity in this depth was lower than in the methanogenesis zone (6–9 cm) but higher than in the upper layer (0–3 cm) of the sediment. The changes in bacterial diversity with depth could be related to the availability of different electron acceptors and of organic matter (Nam et al., 2008). However, there is an overlap between bacterial and archaeal sequences in the middle and the bottom layers (PCoA and Venn diagram), indicating that the environmental conditions are affecting the different processes (sulfate reduction, methanogenesis and AOM). Alpha diversity indexes (Tables 1 and 2) were compared to previous studies conducted only in the upper layer of the sediment of LK using different methods (Schwarz et al., 2007a; Wobus et al., 2003), and showed a similarity in the upper parts of the sediment. However, the deeper layers in this study showed higher diversity and richness than the previous studies previous studies (Nusslein et al., 2001; Schwarz et al., 2007a, 2007b), but diversity and richness indexes were closer to other study sites using 454 sequencing (Hollister et al., 2010; Röske et al., 2012).

The direct mechanism of iron reduction coupled with methane oxidation could be performed by a single microorganism, as methanogens have the ability to reduce iron (Van Bodegom et al., 2004; Bond et al., 2002) although not with methane as the electron donor. This direct mechanism could be performed by unique methanotrophy-like MBG-D (*Thermoplasmata* class) or by MCG/MBG-B (MCG may represent a new archaeal phylum (Lloyd et al., 2013) or a sister lineage to *Thaumarchaeota* (Meng et al., 2014). However, MBG-B is still classified as *Thaumarchaeota*; Marlow et al., 2014), to which some of our sequences were similar. About 5 % of the archaeal sequences in the middle and deep layers were affiliated with MBG-D; however, MCG and MBG-B showed much lower representation and thus are not discussed. Members of the MBG-D have been shown to exist in a variety of freshwater and marine environments (Beal et al., 2009; Borrel et al., 2012), and it is the most widely encountered, uncultured lineage in freshwater lake sediments. Even though their metabolism is unknown, hypotheses about their functionalities are based on the environments in which they were found. Methanogenesis has been suggested, as MBG-D was found in deep lake sediments with high methane concentrations (Borrel et al., 2012), and it was also hypothesized to be involved in AOM, as it was found in AOM zones (Schubert et al., 2011) and in marine seep sediment (Beal et al., 2009). In other environments, in which methane concentrations were low, the utilization of waste products, intermediates, or dead cells by MBG-D was also suggested (Smith et al., 1975). Recently, a single cell genomics study showed that members of MBG-D were capable of exogenous protein degradation in cold anoxic environments (Lloyd et al., 2013).

Another option is a consortium of iron-reducing microbes together with methanotrophs or with methanogens capable of reverse methanogenesis. The well-known iron reducers are *Geobacter* genus; however, only about 1 % of the sequences in the middle and bottom layers or the cores were affiliated with the *Geobacter* genus members. In the deep layer, the most abundant class was Sva0485. Sequences of the SVa485 order were similar to those found in different aquatic environments, but the metabolic functions of members of this order are not clear. *Pelobacter carbinolicus* (Lovley et al., 1995), a member of SVa485, is capable of Fe(III) and sulfur reduction. *Desulfuromonadales*, which was found in our sequences in the deeper parts of the sediment, was shown as S^0 respiring (Pjevac et al., 2014) and may also reduce Fe(III) and Mn(IV) in marine surface sediments (Lovley, 2006). Schwarz et al. (2007a) showed that in the upper part of LK sediment, *Deltaproteobacteria* was one of the dominant classes, and that most of them were affiliated with acetate-oxidizing sulfate-reducing bacteria, that outcompete the acetoclastic methanogens. Even though *Deltaproteobacteria* are best known for their sulfate reduction metabolism, they can shift their metabolism in response to depleted sulfate concentrations (Plugge et al., 2011).

In addition, our results suggest that *Desulfuromonadales* of the *Deltaproteobacteria* class could be also involved in indirect mechanisms of disproportionation of sulfur together with other *Deltaproteobacteria* sulfate reducers. The *dsrA*

functional gene shows that sulfate reducers are present at the same level of the core where *mcrA* functional genes (Fig. 6) of methanogens or methanotrophs are found in the deeper part of the sediment. Additionally, the presence of *Deltaproteobacteria* at the deepest sediment depth and the observed accumulation of acetate with depth (data not shown) could indicate their exploitation of a different metabolic path in the deep sediment than in the upper part of the sediment.

Other options for functioning iron reducers include members of the *Nitrospirae* phylum that increased with depth. Indeed, sequences from our samples were classified as the *Nitrospirales* order in *Nitrospirae* and were most abundant in the bottom layer of the sediment (7 %). Part of our sequences were similar to those found in a previous study (Schwarz et al., 2007b). Using SIP-RNA, Schwarz et al. (2007a) showed not only that *Nitrospirae* were present, but also that they were functionally bioactive. Although *Nitrospirae* is a known nitrate oxidizer (Ehrich et al., 1995), the conditions of this environment suggest that it utilized another metabolic pathway. *Nitrospirae* also include the iron-reducing candidates such as *Magnetobacterium bavaricum* (Spring et al., 1993) and sulfur reducers (Sonne-Hansen and Ahring, 1999). Part of our sequences were aligned against an uncultured clone (98 %) from freshwater sediment which enhanced degradation of phenanthrene and pyrene by amorphous ferric hydroxide (Yan et al., 2012).

The reverse methanogenesis pathway could be carried out by the dominant deep layer methanogens *Methanosaeta*. *Methanosaeta* are acetoclastic methanogens, which are able to grow only on acetate (Jetten et al., 1990). *Methanosaeta* were also shown to be the dominant active methanogens in the upper layer in previous studies of LK (Schwarz et al., 2007a, b) and in other mesotrophic to eutrophic freshwater lakes (Glissman et al., 2004; Koizumi et al., 2003). Yamada et al. (2014) showed that *Methanosaeta* species also have the ability to reduce ferrihydrite with H_2 as the electron source. *Methanosaeta concilii* was the most similar cultured acetoclastic methanogen (96 %) to our sequences which was observed also in the previous study. *Methanosaeta* could perform a different metabolic process or may have been inhibited. The other methanogens that could perform the reverse methanogenesis are from the *Methanomicrobiales* order. In the *Methanolinea* genus of *Methanomicrobiales*, a hydrogenotrophic methanogen was observed at a constant percentage for all depths. The percentage of members of the *Methanoregula* genus, which also contains hydrogenotrophic methanogens, decreased with depth in the core. qPCR analysis of the *mcrA* functional gene of methanogens/anaerobic methanotrophs shows that methanogens were more abundant in the middle layer than in the upper and bottom layers (Fig. 6). ANME were not found in the sediment using specific primers and fluorescence in situ hybridization methods. An additional reason for not finding any ANME sequences in our samples is likely because 454 sequences related to methanogens were found in high percentages and they are probably dominant in the qPCR analysis of *mcrA* gene observed in the deep layer.

The additional indirect mechanism of anaerobic methane oxidation via an oxygenic pathway was shown clearly by the *pmoA* functional gene. The *pmoA* concentration in the deep part of the sediment was higher than in the upper part, indicating an oxygenic pathway (Fig. 6). However, *pMMO* is a homologue enzyme of ammonia monooxygenase and might be sequenced together with *pMMO* (Tavormina et al., 2011). The source of *pMMO* could be *Methylococcales* ($\sim$ 1 %), of *Gammaproteobacteria*, which were observed in the middle and bottom sediment layers. *Methylococcales* are aerobic methanotrophs, which some members were present within the sediments and overlying water column from dysoxic, methane-rich vent and seep systems (Tavormina et al., 2008). The most abundant order in the deep layer was HOC36 (5 %), which is an uncultured *Gammaproteobacteria*. However, when compared to the National Center for Biotechnology Information database, it was found to be closely related to uncultured LK clones (99 %) and to cultured *Methylocaldum* sp. (94 %; Bodrossy et al., 1997), which is a Thermophilic methanotroph isolated from landfill cover soil. However, the bias of *pmoA* with ammonia monooxygenase could be caused by *Thaumarchaeota*, *Betaproteobacteria* or *Nitrospirae*, which were found in all depth.

Thaumarchaeota comprise not only all known archaeal ammonia oxidizers, but also several clusters of environmental sequences representing microorganisms with unknown energy metabolisms (Pester et al., 2011). Members of *Thaumarchaeota* phylum could have monooxygenase-like enzymes that are able to capture methane due to the enzymes' phylogenetic proximities to methane monooxygenases, but that activity requires the necessary downstream metabolic pathway. If they had that ability, they would be good candidates for group of methanotrophic archaea. This indirect pathway can be similar to that found in the NC10 phylum (Zhu et al., 2012), which produces oxygen via the reduction of nitrite and the oxidation of methane, but with iron oxides. Also many bacterial ammonia oxidizer sequences were found in our environment. Ammonium profiles show increase with depth mainly due to decomposition of the organic matter, and theoretically the large amount of ammonium could be oxidized by ferric iron minerals and produce nitrite (Clement et al., 2005). Maybe ammonia monooxygenase can function for ammonium uptake for iron reduction and for methane uptake for oxidation, but that is only speculation. However, no nitrate or nitrite was detected in the deep sediment; moreover, no NC10 phylum (Ettwig et al., 2010) was observed in our sequences.

To summarize, this study attempted to find a correlation between the performed geochemical and microbial profiles in lake sediments. The geochemical data suggest three main depth-related zones where electron acceptor activities take place in the sediment: sulfate reduction, methanogenesis and

a novel, deep iron-driven AOM. The prokaryotic analysis provided clues regarding the microorganisms that may be involved in this novel process and the metabolic paths that occur throughout the microbial assemblage. For AOM via iron reduction to occur, a number of potential pathways and their combinations have been suggested. Orders that become enriched (Sva0485, *Methanosarcinales* and *Nitrospirales*) with depth can be assumed to participate in the AOM process either directly or indirectly. A possible direct process could be through new, currently unknown bacteria/archaea that reduce iron and utilize methane, which may be carried out by a MBG-D as a methanotroph in concert with an iron-reducer-like *Geobacter*. Possible indirect processes could be Fe(III) reduction by sulfide, oxidation of the sulfide to elemental sulfur and other sulfur intermediates and then disproportionation to sulfide and sulfate, and sulfate-driven AOM. However, this process is less likely because ANME were not found. It could also be via reduction of Fe(III) by utilizing H_2, creating a low concentration of H_2 and driving reverse methanogenesis. Fe(III) reduction processes could be carried out by *Nitrospirae* and/or *Deltaproteobacteria*. Members of both groups can reduce iron while in concert with methanogenic *Methanosarcinales*/*Methanomicrobiales*, or can reduce iron with sulfur minerals, creating sulfate (see above) that *Deltaproteobacteria* can utilize while in concert with a MBG-D as a methanotrophic archaea (Schubert et al., 2011). An oxidation of methane coupled to an iron reduction pathway as described by Ettwig et al. (2010) could occur through *Thaumarchaeota* or *Nitrospirae* with a monooxygenase enzyme that can utilize methane while using iron oxides to generate the oxygen needed to oxidize the methane. Further research involving even larger samples of the microbial community and characterizations of more diverse functional genes will provide a better indication of the composition of microbial communities at different depths. Also, microbial and geochemical experiments have the potential to provide more insights into the mechanism of this novel iron-driven AOM.

The Supplement related to this article is available online at doi:10.5194/bg-12-2847-2015-supplement.

Acknowledgements. We would like to thank the editor and reviewers for the helpful and constructive comments. We thank M. Adler for her assistance in the field and in the laboratory. Thanks to the members of Orit's and Ariel's laboratories for all their help. Many thanks to V. Orphan, S. Connon and K. Dawson from Caltech for their help and fruitful discussions. This research was funded by the Water Authority of Israel (O. Sivan and W. Eeckert). E. Kramarsky-Winter is gratefully acknowledged for the thorough scrutiny of the manuscript and for her critical and helpful comments.

Edited by: K. Küsel

References

Adler, M., Eckert, W., and Sivan, O.: Quantifying rates of methanogenesis and methanotrophy in Lake Kinneret sediments (Israel) using pore-water profiles, Limnol. Oceanogr., 56, 1525–1535, 2011.

Beal, E. J., House, C. H., and Orphan, V. J.: Manganese-and Iron-Dependent Marine Methane Oxidation, Science, 325, 184–187, 2009.

Ben-Dov, E., Brenner, A., and Kushmaro, A.: Quantification of sulfate-reducing bacteria in industrial wastewater, by real-time polymerase chain reaction (PCR) using dsrA and apsA genes, Microb. Ecol., 54, 439–451, 2007.

Bligh, E. G. and Dyer, W. J.: A rapid method of total lipid extraction and purification, Can. J. Biochem. Physiol., 37, 911–917, 1959.

Bodrossy, L., Holmes, E. M., Holmes, A. J., Kovács, K. L., and Murrell, J. C.: Analysis of 16S rRNA and methane monooxygenase gene sequences reveals a novel group of thermotolerant, Arch. Microbiol., 168, 493–503, 1997.

Boetius, A., Ravenschlag, K., Schubert, C. J., Rickert, D., Widdel, F., Gieseke, A., Amann, R., Jørgensen, B. B., Witte, U., and Pfannkuche, O.: A marine microbial consortium apparently mediating anaerobic oxidation of methane, Nature, 407, 623–626, 2000.

Bond, D. R., Lovley, D. R., and Methanococcus, A.: Reduction of Fe (III) oxide by methanogens in the presence and absence of extracellular quinones, Environ. Microbiol., 4, 115–124, 2002.

Borowski, W. S., Cagatay, N., Ternois, Y., and Paull, C. K.: Data report: carbon isotopic composition of dissolved CO_2, CO_2 gas, and methane, Blake-Bahama Ridge and northeast Bermuda Rise, ODP Leg 172, Proc. Ocean Drill. Program, Sci. Results, 172, 1–16, 2000.

Borrel, G., Lehours, A.-C., Crouzet, O., Jézéquel, D., Rockne, K., Kulczak, A., Duffaud, E., Joblin, K., and Fonty, G.: Stratification of Archaea in the deep sediments of a freshwater meromictic lake: vertical shift from methanogenic to uncultured archaeal lineages., PLoS One, 7, e43346, 1–14, 2012.

Borrok, D. M., Wanty, R. B., Ridley, W. I., Wolf, R., Lamothe, P. J., and Adams, M.: Separation of copper, iron, and zinc from complex aqueous solutions for isotopic measurement, Chem. Geol., 242, 400–414, 2007.

Chao, A.: Nonparametric Estimation of the Number of Classes in a Population, Scand. J. Stat., 11, 265–270, 1984.

Chao, B. Y. A. and Ma, M.: Stopping rules and estimation for recapture debugging with unequal failure rates, Biometrika, 80, 193–201, 1993.

Chistoserdova, L., Vorholt, J. A., and Lidstrom, M. E.: A genomic view of methane oxidation by aerobic bacteria and anaerobic archaea, Genome Biol., 6, 208.1–208.6, 2005.

Clement, J., Shrestha, J., Ehrenfeld, J., and Jaffe, P.: Ammonium oxidation coupled to dissimilatory reduction of iron under anaerobic conditions in wetland soils, Soil Biol. Biochem., 37, 2323–2328, 2005.

Cline, J. D.: Spectrophotometric determination of hydrogen sulfide In natural waters, Limnol. Oceanogr., 14, 454–458, 1969.

Deutzmann, J. S. and Schink, B.: Anaerobic oxidation of methane in sediments of Lake Constance, an oligotrophic freshwater lake., Appl. Environ. Microbiol., 77, 4429–36, 2011.

Dowd, S. E., Callaway, T. R., Wolcott, R. D., Sun, Y., McKeehan, T., Hagevoort, R. G., and Edrington, T. S.: Evaluation of the bacte-

rial diversity in the feces of cattle using 16S rDNA bacterial tag-encoded FLX amplicon pyrosequencing (bTEFAP), BMC Microbiol., 8, 1–8, 2008.

Eckert, T.: The Influence of Chemical Stratification in the Water Column on Sulfur and Iron Dynamics in Pore Waters and Sediments of Lake Kinneret, Israel, M.Sc. thesis, University of Bayreuth, Germany, 2000.

Eckert, W. and Conrad, R.: Sulfide and methane evolution in the hypolimnion of a subtropical lake: A three-year study, Biogeochemistry, 82, 67–76, 2007.

Edgar, R. C., Haas, B. J., Clemente, J. C., Quince, C., and Knight, R.: UCHIME improves sensitivity and speed of chimera detection, Bioinformatics, 27, 2194–2200, 2011.

Egger, M., Rasigraf, O., Sapart, C. J., Jilbert, T., Jetten, M. S. M., Röckmann, T., van der Veen, C., Banda, N., Kartal, B., Ettwig, K. F., and Slomp, C. P.: Iron-mediated anaerobic oxidation of methane in brackish coastal sediments., Environ. Sci. Technol., 49, 277–283, 2015.

Ehrich, S., Behrens, D., Lebedeva, E., Ludwig, W., and Bock, E.: A new obligately chemolithoautotrophic, nitrite-oxidizing bacterium, Nitrospira moscoviensis sp. nov. and its phylogenetic relationship, Arch. Microbiol., 164, 16–23, 1995.

Ettwig, K. F., Van Alen, T., van de Pas-Schoonen, K. T., Jetten, M. S. M., and Strous, M.: Enrichment and molecular detection of denitrifying methanotrophic bacteria of the NC10 phylum, Appl. Environ. Microbiol., 75, 3656–3662, 2009.

Ettwig, K. F., Butler, M. K., Le Paslier, D., Pelletier, E., Mangenot, S., Kuypers, M. M. M., Schreiber, F., Dutilh, B. E., Zedelius, J., and de Beer, D.: Nitrite-driven anaerobic methane oxidation by oxygenic bacteria, Nature, 464, 543–548, 2010.

Froelich, P. N., Klinkhammer, G. P., Bender, M. L., Luedtke, N. A., Heath, G. R., Cullen, D., Dauphin, P., Hammond, D., Hartman, B., and Maynard, V.: Early oxidation of organic matter in pelagic sediments of the eastern equatorial Atlantic: suboxic diagenesis, Geochim. Cosmochim. Ac., 43, 1075–1090, 1979.

Glissman, K., Chin, K.-J., Casper, P., and Conrad, R.: Methanogenic pathway and archaeal community structure in the sediment of eutrophic Lake Dagow: effect of temperature, Microb. Ecol., 48, 389–399, 2004.

Good, I. J.: The population frequencies of species and the estimation of population parameters, Biometrika, 40, 237–264, 1953.

Hadas, O. and Pinkas, R.: Sulfte-reduction process in sediments of Lake Kinneret, Israel, Hydrobiologia, 235, 295–301, 1992.

Hallam, S. J., Girguis, P. R., Preston, C. M., Richardson, P. M., and DeLong, E. F.: Identification of methyl coenzyme M reductase A (mcrA) genes associated with methane-oxidizing archaea, Appl. Environ. Microbiol., 69, 5483–5491, 2003.

Hallam, S. J., Putnam, N., Preston, C. M., Detter, J. C., Rokhsar, D., Richardson, P. M., and DeLong, E. F.: Reverse methanogenesis: testing the hypothesis with environmental genomics, Science, 305, 1457–1462, 2004.

Hinrichs, K. U., Hayes, J. M., Sylva, S. P., Brewer, P. G., and DeLong, E. F.: Methane-consuming archaebacteria in marine sediments, Nature, 398, 802–805, 1999.

Hoehler, T. M., Alperin, M. J., Albert, D. B., and Martens, C. S.: Field and laboratory studies of methane oxidation in an anoxic marine sediment: evidence for a methanogen-sulfate reducer consortium, Global Biogeochem. Cy., 8, 451–463, 1994.

Holler, T., Wegener, G., Knittel, K., Boetius, A., Brunner, B., Kuypers, M. M. M., and Widdel, F.: Substantial $^{13}C/^{12}C$ and D/H fractionation during anaerobic oxidation of methane by marine consortia enriched in vitro, Environ. Microbiol. Rep., 1, 370–376, 2009.

Hollister, E. B., Engledow, A. S., Hammett, A. J. M., Provin, T. L., Wilkinson, H. H., and Gentry, T. J.: Shifts in microbial community structure along an ecological gradient of hypersaline soils and sediments, ISME J., 4, 829–838, 2010.

Holmkvist, L., Ferdelman, T. G., and Jørgensen, B. B.: A cryptic sulfur cycle driven by iron in the methane zone of marine sediment (Aarhus Bay, Denmark), Geochim. Cosmochim. Ac., 75, 3581–3599, 2011.

Huse, S. M., Welch, D. M., Morrison, H. G., and Sogin, M. L.: Ironing out the wrinkles in the rare biosphere through improved OTU clustering, Environ. Microbiol., 12, 1889–1898, 2010.

Jetten, M. S. M., Stams, A. J. M., and Zehnder, A. J. B.: Acetate threshold values and acetate activating enzymes in methanogenic bacteria, FEMS Microbiol. Lett., 73, 339–344, 1990.

John, S. G. and Adkins, J. F.: Analysis of dissolved iron isotopes in seawater, Mar. Chem., 119, 65–76, 2010.

Kinnaman, F. S., Valentine, D. L., and Tyler, S. C.: Carbon and hydrogen isotope fractionation associated with the aerobic microbial oxidation of methane, ethane, propane and butane, Geochim. Cosmochim. Ac., 71, 271–283, 2007.

Klein, M., Friedrich, M., Roger, a J., Hugenholtz, P., Fishbain, S., Abicht, H., Blackall, L. L., Stahl, D., and Wagner, M.: Multiple lateral transfers of dissimilatory sulfite reductase genes between major lineages of sulfate-reducing prokaryotes, J. Bacteriol., 183, 6028–6035, 2001.

Knittel, K. and Boetius, A.: Anaerobic oxidation of methane: progress with an unknown process., Annu. Rev. Microbiol., 63, 311–334, 2009.

Koizumi, Y., Takii, S., Nishino, M., and Nakajima, T.: Vertical distributions of sulfate-reducing bacteria and methane-producing archaea quantified by oligonucleotide probe hybridization in the profundal sediment of a mesotrophic lake, FEMS Microbiol. Ecol., 44, 101–108, 2003.

Koizumi, Y., Takii, S., and Fukui, M.: Depth-related change in archaeal community structure in a freshwater lake sediment as determined with denaturing gradient gel electrophoresis of amplified 16S rRNA genes and reversely transcribed rRNA fragments, FEMS Microbiol. Ecol., 48, 285–292, 2004.

Lloyd, K. G., Schreiber, L., Petersen, D. G., Kjeldsen, K. U., Lever, M. a., Steen, A. D., Stepanauskas, R., Richter, M., Kleindienst, S., Lenk, S., Schramm, A., and Jørgensen, B. B.: Predominant archaea in marine sediments degrade detrital proteins, Nature, 496, 215–218, 2013.

Lovley, D.: Dissimilatory Fe (III) – and Mn (IV) -Reducing Prokaryotes Microorganisms, in Prokaryotes, 635–658, Springer New York, New York., 2006.

Lovley, D. R.: Dissimilatory Fe(III) and Mn(IV) reduction, Microbiol. Rev., 55, 259–287, 1991.

Lovley, D. R. and Klug, M. J.: Sulfate Reducers Can Outcompete Methanogens at Concentrations Sulfate Reducers Can Outcompete Methanogens Sulfate Concentrationst at Freshwater, Appl. Environ. Microbiol., 45, 187–192, 1983.

Lovley, D. R., Phillips, E. J. P., Lonergan, D. J., and Widman, P. K.: Fe (III) and S0 reduction by Pelobacter carbinolicus, Appl. Environ. Microbiol., 61, 2132–2138, 1995.

Luton, P. E., Wayne, J. M., Sharp, R. J., and Riley, P. W.: The mcrA gene as an alternative to 16S rRNA in the phylogenetic analysis of methanogen populations in landfill, Microbiology, 148, 3521–3530, 2002.

Marlow, J. J., Steele, J. A., Case, D. H., Connon, S. A., Levin, L. A., and Orphan, V. J.: Microbial abundance and diversity patterns associated with sediments and carbonates from the methane seep environments of Hydrate Ridge, OR, Front. Mar. Sci., 1 (October), 1–16, 2014.

McDonald, I. R., Bodrossy, L., Chen, Y., and Murrell, J. C.: Molecular ecology techniques for the study of aerobic methanotrophs., Appl. Environ. Microbiol., 74, 1305–1315, 2008.

Meng, J., Xu, J., Qin, D., He, Y., Xiao, X., and Wang, F.: Genetic and functional properties of uncultivated MCG archaea assessed by metagenome and gene expression analyses, ISME J., 8, 650–659, 2014.

Milucka, J., Ferdelman, T. G., Polerecky, L., Franzke, D., Wegener, G., Schmid, M., Lieberwirth, I., Wagner, M., Widdel, F., and Kuypers, M. M. M.: Zero-valent sulphur is a key intermediate in marine methane oxidation, Nature, 491, 541–546, 2012.

Miyashita, A., Mochimaru, H., Kazama, H., Ohashi, A., Yamaguchi, T., Nunoura, T., Horikoshi, K., Takai, K., and Imachi, H.: Development of 16S rRNA gene-targeted primers for detection of archaeal anaerobic methanotrophs (ANMEs), FEMS Microbiol. Lett., 297, 31–37, 2009.

Nam, Y.-D., Sung, Y., Chang, H.-W., Roh, S. W., Kim, K.-H., Rhee, S.-K., Kim, J.-C., Kim, J.-Y., Yoon, J.-H., and Bae, J.-W.: Characterization of the depth-related changes in the microbial communities in Lake Hovsgol sediment by 16S rRNA gene-based approaches, J. Microbiol., 46, 125–136, 2008.

Niemann, H., Lösekann, T., de Beer, D., Elvert, M., Nadalig, T., Knittel, K., Amann, R., Sauter, E. J., Schlüter, M., and Klages, M.: Novel microbial communities of the Haakon Mosby mud volcano and their role as a methane sink, Nature, 443, 854–858, 2006.

Nishri, A., Imberger, J., Eckert, W., Ostrovsky, I., and Geifman, Y.: The physical regime and the respective biogeochemical processes in the lower water mass of Lake Kinneret, Limnol. Oceanogr., 45, 972–981, 2000.

Nusslein, B., Chin, K. J., Eckert, W., and Conrad, R.: Evidence for anaerobic syntrophic acetate oxidation during methane production in the profundal sediment of subtropical Lake Kinneret (Israel), Environ. Microbiol., 3, 460–470, 2001.

Orphan, V. J., House, C. H., Hinrichs, K. U., McKeegan, K. D., and DeLong, E. F.: Methane-consuming archaea revealed by directly coupled isotopic and phylogenetic analysis, Science, 293, 484–487, 2001.

Orphan, V. J., House, C. H., Hinrichs, K. U., McKeegan, K. D., and DeLong, E. F.: Multiple archaeal groups mediate methane oxidation in anoxic cold seep sediments, P. Natl. Acad. Sci., 99, 7663–7668, 2002.

Pester, M., Schleper, C., and Wagner, M.: The Thaumarchaeota: an emerging view of their phylogeny and ecophysiology, Curr. Opin. Microbiol., 14, 300–306, 2011.

Pjevac, P., Kamyshny, A., Dyksma, S., and Mußmann, M.: Microbial consumption of zero-valence sulfur in marine benthic habitats, Environ. Microbiol., 16, 3416–3430, 2014.

Plugge, C. M., Zhang, W., Scholten, J. C. M., and Stams, A. J. M.: Metabolic flexibility of sulfate-reducing bacteria, Front. Microbiol., 2(May), 1–8, 2011.

Quast, C., Pruesse, E., Yilmaz, P., Gerken, J., Schweer, T., Yarza, P., Peplies, J., and Glöckner, F. O.: The SILVA ribosomal RNA gene database project: improved data processing and web-based tools, Nucleic Acids Res., 41(Database issue), D590–D596, 2013.

Raghoebarsing, A. A., Pol, A., Van de Pas-Schoonen, K. T., Smolders, A. J. P., Ettwig, K. F., Rijpstra, W. I. C., Schouten, S., Damsté, J. S. S., den Camp, H. J. M. O., and Jetten, M. S. M.: A microbial consortium couples anaerobic methane oxidation to denitrification, Nature, 440, 918–921, 2006.

Röske, K., Sachse, R., Scheerer, C., and Röske, I.: Microbial diversity and composition of the sediment in the drinking water reservoir Saidenbach (Saxonia, Germany), Syst. Appl. Microbiol., 35, 35–44, 2012.

Schloss, P. D., Westcott, S. L., Ryabin, T., Hall, J. R., Hartmann, M., Hollister, E. B., Lesniewski, R. a, Oakley, B. B., Parks, D. H., Robinson, C. J., Sahl, J. W., Stres, B., Thallinger, G. G., Van Horn, D. J., and Weber, C. F.: Introducing mothur: open-source, platform-independent, community-supported software for describing and comparing microbial communities, Appl. Environ. Microbiol., 75, 7537–7541, 2009.

Schloss, P. D., Gevers, D., and Westcott, S. L.: Reducing the effects of PCR amplification and sequencing artifacts on 16S rRNA-based studies, PLoS One, 6, e27310, doi:10.1371/journal.pone.0027310, 2011.

Schoell, M.: Multiple origins of methane in the earth, Chem. Geol., 71, 1–10, 1988.

Schubert, C. J., Vazquez, F., Lösekann-Behrens, T., Knittel, K., Tonolla, M., and Boetius, A.: Evidence for anaerobic oxidation of methane in sediments of a freshwater system (Lago di Cadagno), FEMS Microbiol. Ecol., 76, 26–38, 2011.

Schwarz, J. I. K., Eckert, W., and Conrad, R.: Community structure of Archaea and Bacteria in a profundal lake sediment Lake Kinneret (Israel), Syst. Appl. Microbiol., 30, 239–254, 2007a.

Schwarz, J. I. K., Lueders, T., Eckert, W., and Conrad, R.: Identification of acetate-utilizing Bacteria and Archaea in methanogenic profundal sediments of Lake Kinneret (Israel) by stable isotope probing of rRNA., Environ. Microbiol., 9, 223–237, 2007b.

Serruya, C.: Lake Kinneret: the nutrient chemistry of the sediments, Limnol. Oceanogr., 16 (May), 510–521, 1971.

Serruya, C., Edelstein, M., Pollingher, U., and Serruya, S.: Lake Kinneret sediments: nutrient composition of the pore water and mud water exchanges, Limnol. Oceanogr., 19, 489–508, 1974.

Severmann, S., Johnson, C. M., Beard, B. L., and McManus, J.: The effect of early diagenesis on the Fe isotope compositions of porewaters and authigenic minerals in continental margin sediments, Geochim. Cosmochim. Ac., 70, 2006–2022, 2006.

Sivan, O., Adler, M., Pearson, A., Gelman, F., Bar-Or, I., John, S. G., and Eckert, W.: Geochemical evidence for iron-mediated anaerobic oxidation of methane, Limnol. Oceanogr., 56, 1536–1544, 2011.

Sivan, O., Antler, G., Turchyn, a. V., Marlow, J. J., and Orphan, V. J.: Iron oxides stimulate sulfate-driven anaerobic methane oxidation in seeps, P. Natl. Acad. Sci., 111, 4139–4147, 2014.

Smith, P. F., Langworthy, T. A., and Smith, M. R.: Polypeptide nature of growth requirement in yeast extract for Thermoplasma Polypeptide Nature of Growth Requirement in Yeast Extract for Thermoplasma acidophilum, J. Bacteriol., 124, 884–892, 1975.

Sonne-Hansen, J. and Ahring, B. K.: Thermodesulfobacterium hveragerdense sp. nov., and Thermodesulfovibrio islandicus sp. nov., two thermophilic sulfate reducing bacteria isolated from a Icelandic hot spring, Syst. Appl. Microbiol., 22, 559–564, 1999.

Spring, S., Amann, R., Ludwig, W., Schleifer, K. H., van Gemerden, H., and Petersen, N.: Dominating role of an unusual magnetotactic bacterium in the microaerobic zone of a freshwater sediment, Appl. Environ. Microbiol., 59, 2397–2403, 1993.

Stookey, L. L.: Ferrozine-a new spectrophotometric reagent for iron, Anal. Chem., 42, 779–781, 1970.

Tavormina, P. L., Ussler, W., and Orphan, V. J.: Planktonic and sediment-associated aerobic methanotrophs in two seep systems along the North American margin, Appl. Environ. Microbiol., 74, 3985–2995, 2008.

Tavormina, P. L., Orphan, V. J., Kalyuzhnaya, M. G., Jetten, M. S. M., and Klotz, M. G.: A novel family of functional operons encoding methane/ammonia monooxygenase-related proteins in gammaproteobacterial methanotrophs, Environ. Microbiol. Rep., 3, 91–100, 2011.

Thauer, R. K.: Functionalization of methane in anaerobic microorganisms., Angew. Chem. Int. Ed. Engl., 49, 6712–6713, 2010.

Valentine, D. L.: Biogeochemistry and microbial ecology of methane oxidation in anoxic environments: a review, Antonie Van Leeuwenhoek, 81, 271–282, 2002.

Van Bodegom, P. M., Scholten, J. C. M., and Stams, A. J. M.: Direct inhibition of methanogenesis by ferric iron, FEMS Microbiol. Ecol., 49, 261–8, 2004.

Wagner, M., Roger, A. J., Flax, J. L., Brusseau, G. A., and Stahl, D. A.: Phylogeny of dissimilatory sulfite reductases supports an early origin of sulfate respiration, J. Bacteriol., 180, 2975–2982, 1998.

Whiticar, M. J.: Carbon and hydrogen isotope systematics of bacterial formation and oxidation of methane, Chem. Geol., 161, 291–314, 1999.

Wobus, A., Bleul, C., Maassen, S., Scheerer, C., Schuppler, M., Jacobs, E., and Röske, I.: Microbial diversity and functional characterization of sediments from reservoirs of different trophic state, FEMS Microbiol. Ecol., 46, 331–347, 2003.

Yamada, C., Kato, S., Kimura, S., Ishii, M., and Igarashi, Y.: Reduction of Fe(III) oxides by phylogenetically and physiologically diverse thermophilic methanogens, FEMS Microbiol. Ecol., 89, 637–645, 2014.

Yan, T., Ye, Q., Zhou, J., and Zhang, C. L.: Diversity of functional genes for methanotrophs in sediments associated with gas hydrates and hydrocarbon seeps in the Gulf of Mexico, FEMS Microbiol. Ecol., 57, 251–259, 2006.

Yan, Z., Song, N., Cai, H., Tay, J.-H., and Jiang, H.: Enhanced degradation of phenanthrene and pyrene in freshwater sediments by combined employment of sediment microbial fuel cell and amorphous ferric hydroxide, J. Hazard. Mater., 199-200, 217–225, 2012.

Ye, W., Liu, X., Lin, S., Tan, J., Pan, J., Li, D., and Yang, H.: The vertical distribution of bacterial and archaeal communities in the water and sediment of Lake Taihu, FEMS Microbiol. Ecol., 70, 107–120, 2009.

Zhu, B., van Dijk, G., Fritz, C., Smolders, A. J. P., Pol, A., Jetten, M. S. M., and Ettwig, K. F.: Anaerobic oxidization of methane in a minerotrophic peatland: enrichment of nitrite-dependent methane-oxidizing bacteria, Appl. Environ. Microbiol., 78, 8657–8665, 2012.